

# Diffraction optics applied to eyepiece design

Michael D. Missig and G. Michael Morris

Eyepieces often limit the overall optical performance of visual instruments and, because of the wide field-of-view and high-performance requirements, they present a well-known difficult design problem. Improvement of existing eyepieces is limited with the use of conventional design variables. We have designed and fabricated a hybrid diffractive–refractive wide-field ( $>60^\circ$ ) eyepiece that offers significant improvements over existing conventional eyepieces. The hybrid eyepiece consists of only three common-crown refractive elements and weighs 70% less than an Erfle-type eyepiece, while having enhanced optical performance such as a 50% decrease in pupil spherical aberration and a 25% reduction in distortion. Experimental modulation transfer function results are in excellent agreement with the theoretical performance.

## 1. Introduction

Eyepieces play an important role in many types of optical systems with applications in entertainment systems, sports optics, medical instruments, military systems, and surveillance equipment. The eyepiece is often the limiting factor in the overall optical performance of the instrument and, because of the requirements for sufficient eye relief and high performance, it presents a challenging design problem. Improvement of existing eyepiece designs is limited with the use of conventional design variables. By the introduction of a new technology—diffractive optics—to eyepiece design, the performance of today's eyepieces can be enhanced. Advantages of a diffractive optics solution to eyepiece design include smaller lens curvatures, higher numerical-aperture achromats, and reductions in the number of elements, overall weight, and system cost, as well as an increase in optical performance compared with an all-refractive eyepiece design.

We have designed several diffractive–refractive hybrid eyepieces for use in wide-field visual instruments. These eyepieces offer increased optical performance compared with all-refractive conventional eyepieces. These benefits include improved imaging and physi-

cal features, such as reduced overall size, weight, and amount of glass.

The design of improved wide-angle eyepieces can be limited by the use of conventional optics. Classical eyepiece design and the implementation and benefits of diffractive optics to this problem are presented in Section 2. The design methodology and the optimization procedure are also discussed in Section 2. In Section 3 we describe two diffractive–refractive eyepieces with a performance comparable with or better than the well-known Erfle eyepiece. In Section 4 an analysis of the effects of the diffraction efficiency of the diffractive element on the imaging performance of the eyepiece is presented. One of the diffractive–refractive eyepieces has been fabricated as a 20-mm focal length (FL) eyepiece. Experimental results for the modulation transfer functions (MTF's) of the hybrid eyepiece and a six-element Erfle eyepiece are presented in Section 5.

## 2. Eyepiece Design

### A. Conventional Refractive Eyepieces

Eyepieces are unique optical systems that differ greatly in function and design from imaging objective lenses. The requirements for the design of an eyepiece are a direct result of its unique functions. An eyepiece is required to present a magnified image of a near object or secondary image—an internal image of an objective subsystem—at a comfortable distance for the human eye. Furthermore, an eyepiece must provide sufficient eye relief for the user of the optical system. From each of these functions come many design characteristics of eyepieces. In terms of uniqueness, the last design requirement is of the greatest signifi-

---

When this work was performed, the authors were with the Institute of Optics, University of Rochester, Rochester, New York 14627. M. D. Missig is now with Optikos Corporation, 286 Cardinal Medeiros Avenue, Cambridge, Massachusetts 02141.

Received 23 August 1994; revised manuscript received 21 November 1994.

0003-6935/95/142452-10\$06.00/0.

© 1995 Optical Society of America.

cance. In providing eye relief for the user, an eyepiece must provide a well-imaged, external exit pupil. Therefore the eyepiece must provide adequate correction for the imaging aberrations and simultaneously be well corrected for the pupil aberrations as well.

By having an external aperture stop, a wide field of view (FOV), and requirements for optical correction of both imaging and pupil aberrations, eyepiece design has become a well-known difficult design problem. The requirement for eye relief combined with that for a large FOV, results in large aperture elements (in comparison with the overall eyepiece aperture). Because the aperture stop is external to the eyepiece, the element apertures increase as the FOV is increased, while the eye relief is maintained constant. The same occurs if the FOV is fixed while the eye relief is increased. Therefore it is difficult to design an eyepiece with both a long eye relief and a wide field. Additionally, the inevitable increase in the element diameters aggravates the monochromatic aberrations. Another unfortunate characteristic is that the external stop location eliminates the symmetry of the optical system about the principal ray, which would help to reduce coma, distortion, and lateral color. Often the lateral color in an eyepiece is so strong that each positive element in the eyepiece is achromatized with a dispersive, negative element. Furthermore, little can be done to reduce the field curvature in an eyepiece because of its relatively short FL.<sup>1</sup> Strong meniscus elements placed near the focal plane are often used to combat this problem.<sup>2</sup> With all these design issues, well-corrected, conventional eyepieces have complex, multielement forms<sup>3</sup>; this significantly reduces their desirability in a number of situations. In such cases, optical performance is often sacrificed to satisfy weight or cost requirements, and improvements of classical eyepieces in terms of optical performance and physical size have been scarce. The well-known Erfle eyepiece<sup>4</sup> is considered to be a very good compromise of optical performance with size, weight, and number of elements for wide-field use and is probably the most commonly used wide-field eyepiece.<sup>5</sup> The Erfle eyepiece described in the 1923 patent<sup>4</sup> is shown in Fig. 1 and is used as a design comparison for the hybrid designs presented here.

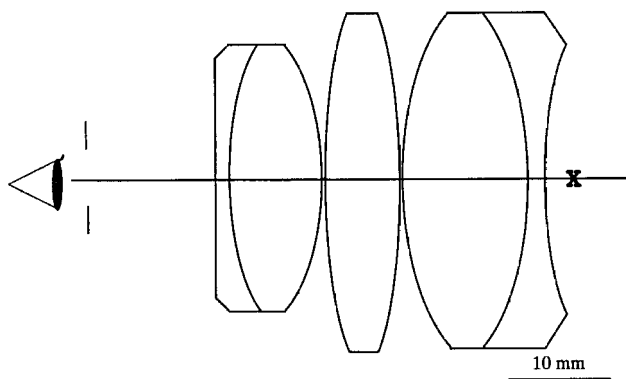


Fig. 1. Five-element Erfle eyepiece, 60° FOV.

## B. Wide-Angle, Hybrid Diffractive–Refractive Eyepieces

With its unique features and characteristic design constraints, eyepiece design is a difficult task. It has even been suggested that further design work attempting improvements of existing eyepieces may be fruitless.<sup>6</sup> This is largely due to the inherent limitations imposed by conventional refractive optics applied to this problem. The first of these disadvantages is the task of color correction. The powers of the color-correcting elements in conventional eyepiece designs are such that excessive size and weight are added to the optical system. Furthermore the opposing converging powered elements are consequently also strong; thus conventional eyepiece designs tend to have strong surface curvatures, which adversely affect the monochromatic aberrations. In fact, the steep surface curvatures induced by the negative color-correcting elements further aggravate the correction of distortion, pupil spherical aberration, and astigmatism, which is already complicated by the external stop and wide FOV.

As a new design variable, diffractive optics offers a number of features that are beneficial to eyepiece design. For example, the effective dispersion of diffractive lenses is opposite in sign to that of refractive elements.<sup>7</sup> For this reason, color-corrected hybrid eyepieces may be designed with all positive elements. This feature is particularly useful for eyepiece design, as the surface curvatures of the refractive elements in the design can then be significantly reduced compared with the surface curvatures in all-refractive, conventional eyepieces. As a result, the monochromatic aberrations are easier to correct.

Eyepieces consist of a close grouping of mostly strongly positive-powered elements with a combined short FL. Therefore field curvature is difficult to reduce in conventional eyepieces, and often overcorrected astigmatism is introduced to flatten the sagittal field, while allowing the tangential field to curve slightly backward. (Note that when rays are traced from long conjugate to short, the tangential field is backward curving; when rays are traced from short to long, the opposite is the case.) A desirable attribute of diffractive lenses is that they contribute no Petzval field curvature.<sup>8–10</sup> In the hybrid eyepieces described herein, there are no field-flattening, negative elements, yet on the other hand the refractive surfaces are weaker (than those in conventional eyepieces) and the diffractive elements introduce no Petzval field curvature. These effects offset each other to result in a slightly reduced field curvature. In addition, when fabricated as surface-relief structures, diffractive lenses can offer considerable size and weight reductions. Along with these features, diffractive optics can also be used to shape the emerging wave front to help correct the monochromatic aberrations.<sup>10</sup>

To reduce the remaining field aberrations, higher-order terms in the phase profile of the diffractive lenses in the hybrid eyepieces have been optimized. Values of distortion are typically severe in eyepieces;

the type of distortion found in eyepieces is the pincushion or positive type.<sup>1</sup> It is not unusual to find 8%–12% distortion in eyepieces covering 60°–70° full FOV.<sup>5</sup> The amount of this aberration would be unacceptable in standard photographic lenses, yet it is tolerated in eyepieces in part because of its difficulty to correct and also because the eye–brain system is a forgiving image processor. Not uncommon in visual instruments, the edge of the field is used to orient the user and to locate objects.<sup>5</sup> Objects seen at the edge of the field are then brought to the center of the FOV with better detail. Aspheric surfaces are used in some cases to correct the distortion in wide-field eyepieces.<sup>5</sup> This can be an expensive, undesirable option to improve the quality of the optical device if all surfaces are glass. Consequently, distortion is often left uncorrected in many eyepieces.<sup>11</sup> Distortion can be significantly reduced with diffractive optics, as the introduction of an aspheric term into the diffractive lens typically adds little or no difficulty to the fabrication of the element.

The correction of pupil spherical aberration is important in visual instruments in which an exit pupil must remain stationary so that no unwanted vignetting is introduced. To calculate the amount of pupil spherical aberration, a bundle of chief rays are traced from the center of the entrance pupil, typically at the system objective, through the eyepiece, and the longitudinal aberration is evaluated at the exit pupil. (Note that a chief ray is defined as a geometric ray originating from the object and passing through the center of the entrance pupil.) As the eyepiece usually comprises a closely gathered group of convergent elements, these chief rays suffer from undercorrected spherical aberration. The effect of this aberration can be a zonal vignetting of the field, often known as a kidney bean effect.<sup>11</sup> The user will typically shift his or her eye back and forth, along the optical axis, to capture the remaining unvignetted portions of the field. As this is done, the previously unshadowed portions of the field will now become vignetted.

Pupil spherical aberration and distortion are closely related in eyepieces.<sup>2</sup> As described in the previous paragraph, in the case of undercorrected pupil spherical aberration, the chief ray is bent at progressively steeper angles as the field angle increases. Hence, with the larger chief ray angles, the corresponding part of the image field will be magnified larger than expected. This is known as pincushion distortion, which is the type of distortion found in eyepieces.

Prior work on telescopic and similar visual instruments that incorporate diffractive elements includes a zone-plate telescope,<sup>12</sup> a simple diffractive-doublet eyepiece design,<sup>13</sup> and a hybrid, diffractive–refractive telescope in which a diffractive eyepiece compensates for the residual color in the refractive objective.<sup>14</sup> These were all first-order designs in which monochromatic aberrations were left uncorrected. Recently there has been work done in the area of hybrid diffractive–refractive magnifiers.<sup>15,16</sup> Magnifiers and eyepieces are often categorized as identical systems,

although there are significant differences both in function and in characteristic design configurations.<sup>17</sup> Magnifiers, which are commonly used in night-vision goggles and similar devices, typically view a screen image. In that case there is no requirement for pupil imaging as in the case for eyepieces used in instruments such as telescopes or binoculars. Eyepieces must be well corrected for longitudinal displacements of the eye along the optical axis, whereas magnifiers need to accommodate for eye shifts in the lateral direction. Furthermore, magnifier image screens tend to be quasi-monochromatic, and therefore the color-correction requirements are not as difficult to achieve; however, eyepieces tend to work over a broadband spectrum. Often wide-angle eyepieces, such as the Erfle eyepiece, have been used as magnifiers in head-mounted systems; but the use of a magnifier as an eyepiece is not usually sufficient. A binocular magnifier, which is to be viewed with both eyes, that employed one diffractive surface was recently reported.<sup>15</sup> Additionally, a diffractive–refractive doublet was designed for use as a magnifier,<sup>16</sup> in which a diffractive element was designed on a curved substrate with the second surface an aspheric.

### 3. Design Examples—Diffractive-Refractive Eyepieces

Two examples of hybrid diffractive–refractive, wide-field eyepieces are presented that demonstrate the effectiveness of diffractive optics in providing improved performance eyepieces with fewer elements than existing, conventional eyepiece designs. Comparisons with a common wide FOV eyepiece design are presented. For eyepiece comparisons, the Erfle eyepiece provides a good benchmark for both performance and size. An Erfle eyepiece<sup>4</sup> (Fig. 1) consists of a five-element design, with strong positive and negative elements, covering up to a 60° apparent FOV (i.e., the FOV on the eye side of the eyepiece.) The two hybrid eyepiece designs are compared with the Erfle eyepiece; all three designs have equivalent FL's,  $f$ -numbers, and FOV's. In Figs. 1 and 2 the eye is positioned at the exit pupil location, and **X** marks the location of the image plane.

With the use of diffractive optics as an added tool, the objective was to design a three-refractive-element eyepiece (employing one or two diffractive elements) that had an optical performance at least equivalent to the Erfle. In the design process several constraints, such as no negative or thick elements, were applied to the problem so as to reduce the weight and the size of the eyepiece. It seemed reasonable that a three-refractive-element design (plus one or two diffractive lenses) would offer considerable weight and size reduction and also have a sufficient number of design variables to yield a well-corrected eyepiece. The first step in the design process of the hybrid eyepiece was to use the same distribution of powers as is used in the Erfle, replacing the flint elements with diffractive lenses. The first hybrid eyepiece design, shown in Fig. 2(a), consists of three refractive lenses and two

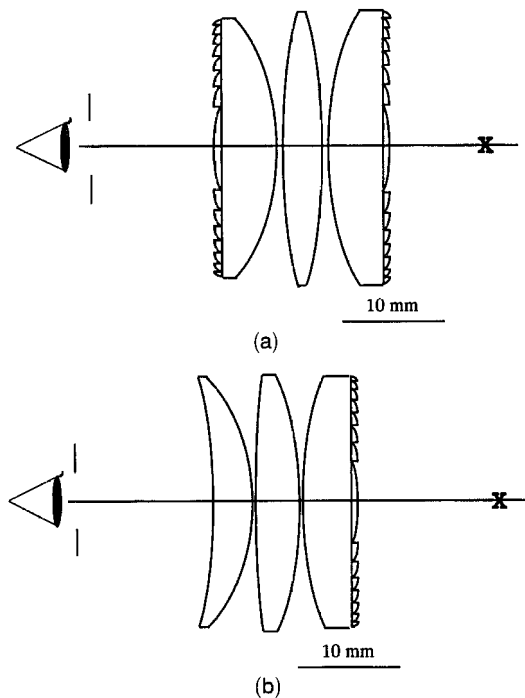


Fig. 2. Wide-angle, hybrid diffractive-refractive eyepieces. (a) Three refractive elements, two diffractive elements, (b) three refractive elements, one diffractive element; 60° FOV. Note that refractive elements are drawn to scale, but diffractive elements are drawn schematically.

diffractive surfaces. Two of the refractive elements have a planar side to which the diffractive elements are directly mounted. Planar substrates were chosen for the diffractive optical elements of both hybrid eyepiece configurations to simplify fabrication. The initial layout was as follows: create two hybrid diffractive-refractive achromats with overall powers equivalent to the two refractive doublets in the Erfle design, therefore maintaining the power distribution in each of the three lens groups. The constructional parameters were subsequently adjusted to maintain proper first-order features, i.e., total FL, telecentricity, and a sufficient eye relief. In the design and analysis of the eyepieces, rays were traced backwards through the system. In other words, rays were traced from infinity from the eye side of the eyepiece through the lens to the focal plane of the lens. Under actual usage, the eyepiece actually views an object or image located at or very near the focal plane of the eyepiece.

The first design used the same glasses as the crown glasses in the original Erfle design. The distribution of element powers was optimized for color correction, while the surface curvatures were initially optimized to flatten the sagittal field. Later in the design process, pupil spherical aberration and distortion were introduced into the merit function as well. Given the limited number of refractive variables, the most effective remaining variables to bring these aberrations under control were the higher-order terms in the phase polynomials of the diffractive lenses.

A compromise was found between optimal monochromatic aberration correction and sufficient lateral color reduction. With the use of diffractive surfaces to correct both color and certain monochromatic aberrations, often a stable balance can be difficult to find. The diffractive elements in the first eyepiece are relatively weak; the two elements together comprise approximately 8% of the total eyepiece power.

In the design of the second hybrid eyepiece, Fig. 2(b), the motivating factor was to have the diffractive surfaces internal to the visual system, such that the diffractive lenses would be environmentally protected, i.e., none on the eye side. Additionally, the elimination of the second diffractive surface was explored (as a result, this diffractive-element reduction would increase the overall diffraction efficiency of the system). Several positions of the diffractive surface [which is external in the eyepiece in Fig. 2(a)] were investigated with the best configuration shown in Fig. 2(b).

In some designs, we placed an external window to cover the front diffractive surface; unfortunately this also reduces the effective eye relief. We also attempted a design form with a diffractive element on the inside surface of this window, although this solution offered negligible gains in performance. Furthermore, the cover-plate solution is essentially a four refractive-element lens. In another design configuration, the first hybrid doublet from the design shown in Fig. 2(a) was reversed in an attempt to shield the diffractive element environmentally. This configuration had the effect of worsening the field aberration correction. Even with the use of the higher-order terms in the phase polynomial (aspheric terms) to balance out the induced aberrations from this form, a design with a performance comparable with that in the eyepiece depicted in Fig. 2(a) could not be obtained.

The solution to the question of the best position of the diffractive surface seems to be at the last surface. The surface nearest the focal plane, i.e., the surface furthest from the eye, tends to offer good correction when it is plane or nearly plane; this is because its shape is concentric to the entrance pupil. For this reason, it is naturally the best place for a diffractive lens, as was the case in the first design as well. Because the color-correcting powers of the diffractive elements in the first design were also quite weak, it seemed reasonable to try to combine their powers together and use a single diffractive lens. This design left the first glass surface to vary during optimization; the front refractive surface of the eyepiece is actually a strong variable for both extending the eye relief and reducing distortion and pupil spherical.

The lens design prescription data for the two hybrid eyepieces depicted in Figs. 2(a) and 2(b) are listed in Tables 1 and 2, respectively. The curvatures of the refractive elements of the hybrid designs, Figs. 2(a) and 2(b), are significantly less than those of the Erfle eyepiece, Fig. 1. Furthermore, with the

Table 1. Lens Prescription Data for Hybrid Eyepiece shown in Fig. 2(a)<sup>a</sup>

Surface	Radius (mm)	Thickness (mm)	Glass	Semidiameter (mm)
1 <sup>b</sup>	0	15.81185	BAK2	15.5
2	-24.17843	6.77651		15.5
3	78.01601	0.67765	BK7	16.0
4	-78.01601	4.51767		16.0
5	36.92287	0.67765	BAK2	16.0
6 <sup>c</sup>	0	6.83163		16.0

<sup>a</sup>20-mm FL.

<sup>b</sup>Diffraction lens 1 phase coefficients:  $s_1 = -0.0011802$ ,  $s_2 = 2.789686 \times 10^{-6}$ .

<sup>c</sup>Diffraction lens 2 phase coefficients:  $s_1 = -5.789915 \times 10^{-4}$ .

use of diffractive elements in the design, the necessity for exotic glass use has been eliminated. In the two hybrid eyepieces, only common glasses were used: the eyepiece in Fig. 2(a) comprised BK-7 and BAK-2, and the eyepiece shown in Fig. 2(b) comprised BK-7 entirely.

In the design of the eyepieces, the Sweatt model was used to set up the initial forms of the diffractive lenses with an index of refraction at the center wavelength equal to 10,000.<sup>18</sup> The wavelengths used during optimization were  $\lambda = 588$  nm,  $\lambda = 486$  nm, and  $\lambda = 656$  nm. In the final optimization and analysis stages, the phase model of the diffractive lenses was used to characterize the lens more accurately. In this case, a rotationally symmetric phase polynomial was used to describe the diffractive surface:

$$\varphi(r) = \frac{2\pi}{\lambda} (s_1 r^2 + s_2 r^4 + s_3 r^6 + s_4 r^8 + \dots) \quad (1)$$

Comparisons of design performance for the hybrid, wide-angle eyepiece in Fig. 2(b) and for the Erfle eyepiece in Fig. 1 are shown in Figs. 3–5. Important figures of merit to compare in eyepiece designs are distortion, pupil spherical aberration, and lateral color. The aberration corrections of the two hybrid eyepieces are similar, whereas the performance of the eyepiece in Fig. 2(b) is slightly better. All three eyepieces are scaled to a FL of unity, opened to an aperture of  $f/2.5$ , and have a 60° FOV.

Table 2. Lens Prescription Data for Hybrid Eyepiece shown in Fig. 2(b)<sup>a</sup>

Surface	Radius (mm)	Thickness (mm)	Glass	Semi-Diam (mm)
1	-54.09807	15.81185	BK7	12.8
2	-19.42586	3.92929		12.8
3	157.28572	0.1	BK7	13.0
4	-43.01555	4.03694		13.0
5	34.97115	0.24401	BK7	13.0
6 <sup>b</sup>	0	5.38258		13.0

<sup>a</sup>20-mm FL.

<sup>b</sup>Diffraction lens phase coefficients:  $s_1 = -0.001945$ ,  $s_2 = 4.121263 \times 10^{-6}$ .

The distortion plots for the two eyepieces (Fig. 3) show that the hybrid exhibits approximately 6% distortion at 30° half FOV, whereas the Erfle eyepiece has approximately 8% distortion at the equivalent field angle. (Note that the sign of distortion aberration changes when the system is analyzed long conjugate to short.) Likewise, the pupil spherical aberration of the hybrid eyepiece is significantly reduced compared with the Erfle eyepiece. In Fig. 4, longitudinal pupil spherical aberration of the exit pupil is plotted versus field angle for three wavelengths, 486, 588, and 656 nm. The polychromatic performance is shown for the purpose of demonstrating the feature that the hybrid is well corrected for chromatic variation of this aberration. Diffractive visual systems in the past have exhibited significant variation of pupil location with wavelength changes.<sup>11</sup> The decreased pupil spherical aberration in the hybrid eyepiece aids the viewer in reducing vignetting and maintaining a stationary exit pupil.

In Fig. 5, the chromatic variation of magnification error, i.e., lateral or transverse color, is plotted for the Erfle and the hybrid eyepieces. Note that the hybrid eyepiece has improved color correction throughout at least 70% of the FOV, with a performance comparable with the Erfle at the edge of the field.

There are additional first-order and physical benefits of the hybrid eyepieces compared with the Erfle eyepiece, as indicated in Table 3. In summary, the hybrid eyepieces offer significant weight and size reductions, while also offering increased eye relief, increased working distance or back focal length, less expensive glasses, more compact eyepieces, and improved optical performance (such as reduced distortion, pupil spherical aberration, and better color correction).

#### 4. Diffraction Efficiency

Diffractive lenses, unlike conventional optics, can produce more than one image because of the multiple diffracted orders of the lens. These other diffracted orders can reduce the resolution of an optical system by introducing unwanted background light at the image plane. Nonunity diffraction efficiency can occur because of fabrication errors in the lens as well as changes in wavelengths from the peak (or design) wavelength, as predicted by scalar theory. Furthermore, as the zone spacing to wavelength ratio decreases below approximately 10 or so, significant deviations in efficiency from those predicted by scalar models can be expected. Often the outer zones at the edge of the diffractive lens have the smallest spacings across the aperture of the element. Therefore diffractive lenses with low  $f$ -numbers are limited by the close zone spacings at the edge of the lens, which can severely reduce the diffraction efficiency compared with that predicted by scalar theory.

The integrated efficiency,  $\eta_{int}$ , has been shown to provide a useful figure of merit to describe the effects

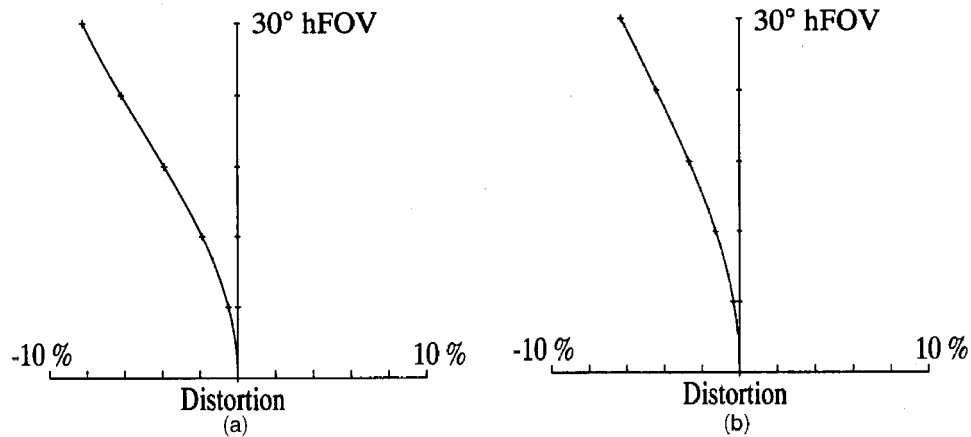


Fig. 3. Percent distortion versus field angle for (a) Erfle eyepiece, (b) hybrid eyepiece in Fig. 2(b).

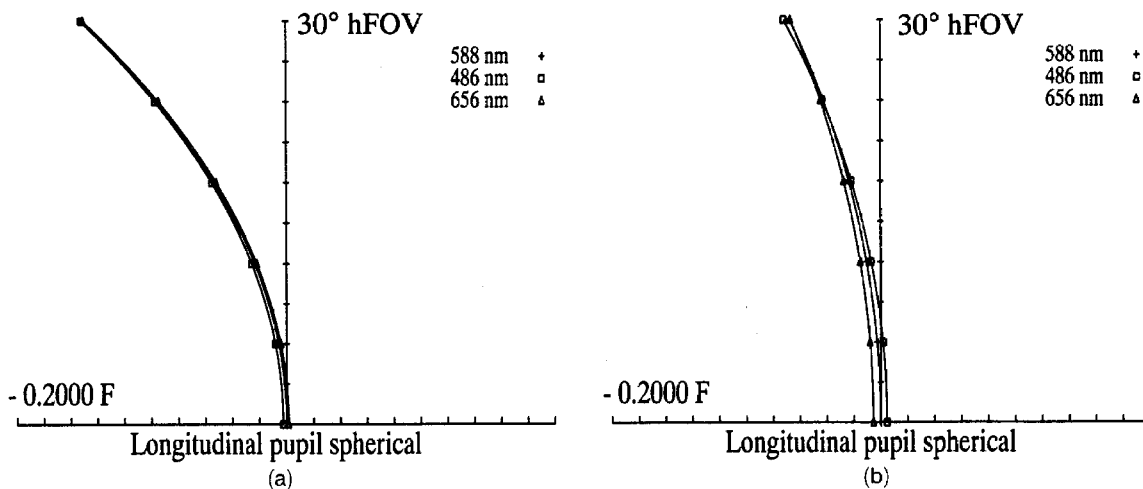


Fig. 4. Longitudinal pupil spherical aberration (486, 588, 656 nm) versus field angle for (a) Erfle eyepiece, (b) hybrid eyepiece in Fig. 2(b). The data are scaled by the FL (F) of the eyepiece.

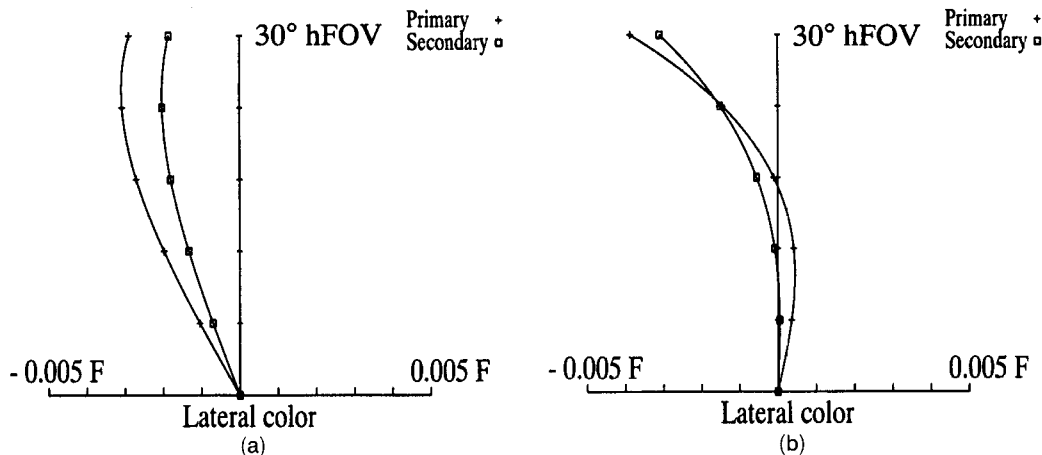


Fig. 5. Primary lateral color and secondary lateral color versus field angle for (a) Erfle eyepiece, (b) hybrid eyepiece in Fig. 2(b). The data are scaled by the FL (F) of the eyepiece.

of nonunity diffraction efficiency on the performance of diffractive lenses.<sup>19</sup> The integrated efficiency describes the deterministic loss of energy from the desired diffracted order into the additional back-

ground diffracted orders and does not include the effects of random surface scatter. The integrated efficiency has been defined<sup>19</sup> as the pupil-averaged value of the local diffraction efficiency,  $\eta_{\text{local}}$ :

**Table 3. Characteristics and Performance Features for the Erfle Eyepiece and the Wide-Angle Hybrid Diffractive–Refractive Eyepieces in Figs. 2(a) and 2(b)<sup>a</sup>**

Eyepiece	Petzval				
	Radius/FL	Weight	OAL/FL	ER/FL	BFL/FL
Erfle	-1.516	1.00	1.48	0.58	0.46
Hybrid Fig. 2(a)	-1.528	0.61	0.97	0.79	0.64
Hybrid Fig. 2(b)	-1.609	0.31	0.68	0.79	0.79

<sup>a</sup>The following data are given: the ratio of the Petzval field radius to the eyepiece FL, the weight of the glass of the eyepieces normalized by the Erfle glass weight, the ratio of the overall length (OAL) (first physical surface to last surface) to the eyepiece FL, the ratio of eye relief (ER) to the eyepiece FL, and the ratio of the back FL (BFL) to the eyepiece FL.

$$\eta_{\text{int}} = \frac{1}{A_{\text{pupil}}} \int_{-\infty}^{\infty} \int_{-\infty}^{\infty} \eta_{\text{local}}(u, v) du dv, \quad (2)$$

where  $A_{\text{pupil}}$  is the exit pupil area and  $\eta_{\text{local}}$  is the local efficiency of the diffractive lens for a given aperture coordinate. Buralli and Morris showed that the integrated efficiency serves as a scaling factor for the MTF of the lens.<sup>19</sup>

The effects of nonunity diffraction efficiency of the eyepiece optical system can be seen by comparing the diffraction efficiency of the diffractive lens with the spectral sensitivity of the detector system, i.e., the human eye. The human eye is the final judge of the performance of a visual instrument, and in many aspects it can be a tolerant detector. With a judicious choice of blaze height for the diffractive lens, a good match can be made for the efficiency of a diffractive lens and the relative sensitivity of the eye for a given set of illumination conditions.

A comparison of the relative sensitivity of the human eye under photopic conditions and the scalar diffraction efficiency of a quadratic profile diffractive lens with peak efficiency at  $\lambda_0 = 0.555 \mu\text{m}$  is shown in Fig. 6. The diffraction efficiency for a continuous-blaze diffractive lens for the  $m$ th order is given by<sup>20</sup>

$$\eta_m = \text{sinc}^2(\alpha - m). \quad (3)$$

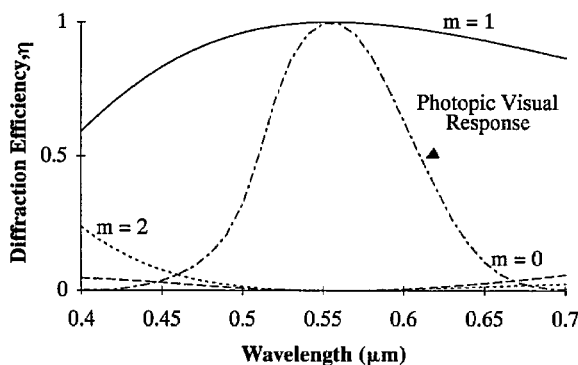


**Fig. 6.** Diffraction efficiency of a diffractive lens with peak efficiency at  $\lambda_0 = 0.555 \mu\text{m}$  for the  $m = 0, 1, 2$  diffracted orders and the photopic visual response of the human eye.

The parameter  $\alpha$  allows for efficiency calculations that are due to wavelength changes:

$$\alpha = \left( \frac{\lambda_0}{\lambda} \right) \left[ \frac{n(\lambda) - 1}{n(\lambda_0) - 1} \right], \quad (4)$$

where  $n(\lambda)$  is the index of refraction as a function of the incident wavelength for the diffractive lens material. The scalar peak efficiency is 100% at the center wavelength  $\lambda_0$  in the  $m = 1$  order and decreases for other wavelengths. As the wavelength of the light is increased and more light is diffracted into the  $m = 0$  order (undiffracted light), the eye simultaneously becomes less sensitive to that light than to the light diffracted around the peak wavelength. A similar decrease in eye sensitivity occurs as the light is further detuned to shorter wavelengths, for which more light is diffracted into the second order ( $m = 2$ ). Therefore the effects of undiffracted light may be offset by the tolerance of the human eye and the brain as the detector and image processor. Additionally, a different blaze height can be chosen [Eq. (4)] to accommodate a particular system condition or application.

## 5. Experimental Results

The eyepiece depicted in Fig. 2(b) was fabricated for experimental comparison with the Erfle eyepiece. To construct the surface profile, physical specifications were generated from the phase function of the diffractive lens. The phase profile of the lens is given by Eq. (1), where the phase coefficients are specified in Table 2. The zone radii were determined by the solution of the equation for  $2\pi$  phase transitions. These radii are then used to specify the construction of a master element.

The master diffractive element was fabricated with a laser pattern generator, and replicas were made from the master element.<sup>21</sup> The diffractive lens in the eyepiece operates at an  $f$ -number of  $f/10$  and has a fourth-order aspheric profile in the phase poly-

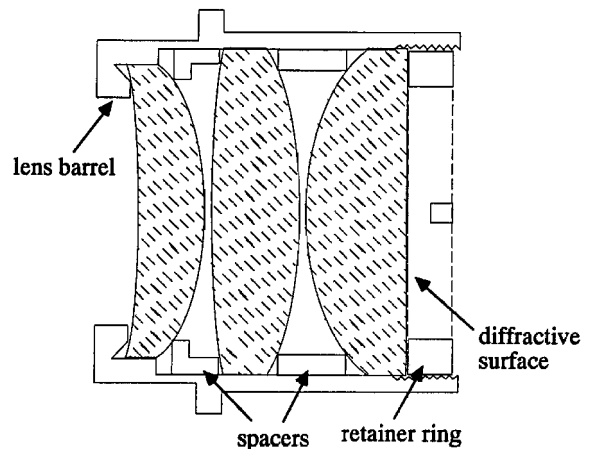


**Fig. 7.** Schematic diagram of the mounted hybrid wide-field eyepiece depicted in Fig. 2(b).

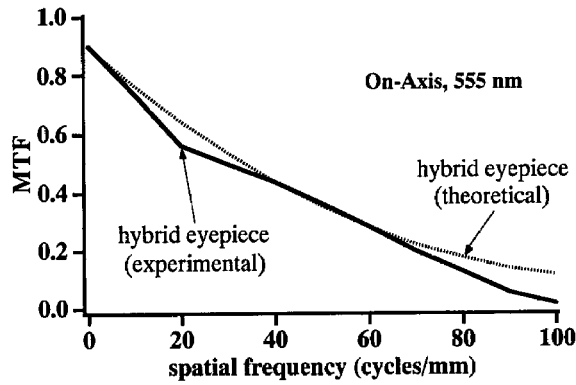


Fig. 8. Experimental and theoretical on-axis MTF's for hybrid eyepiece in Fig. 2(b) with  $\lambda = 555$  nm.

mial that defines the diffractive surface (see the specifications listed in Table 2). The minimum zone spacing of the lens is approximately  $25 \mu\text{m}$ , which occurs at a radial position of approximately 70% of the full aperture.

A tolerance analysis was performed to predict the performance changes expected with fabrication-alignment errors. The tolerancing of the refractive elements was a standard analysis, including surface power and irregularity, element thickness and wedge errors, and refractive-index errors. Additionally, airspace changes and element tilt and decenter errors were also included. For the diffractive element, the most critical fabrication error was the decenter between the optical axes of the diffractive lens and the refractive lens. Tilt in the diffractive element is also important, but this specification can usually be added into the wedge error tolerance value for the plano-convex refractive-element substrate. The alignment accuracy required for the decenter of the diffractive element with respect to the refractive substrate was determined to be less than  $70 \mu\text{m}$ . The merit used to determine the tolerance budget was rms spot size. With the allowable tolerance values, the predicted, worst-case performance decrease was 1%–2% in on-axis rms spot size.

A schematic diagram of the mounted hybrid eyepiece lens is shown in Fig. 7.

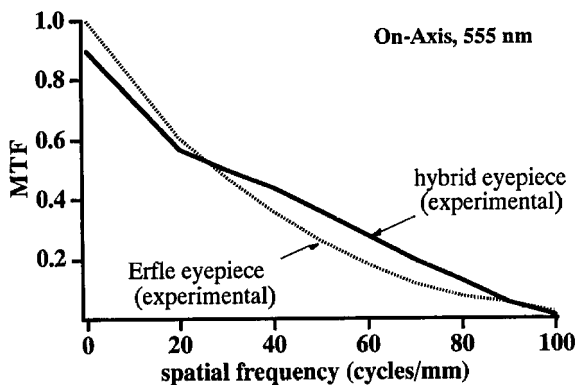


Fig. 9. Experimental on-axis MTF's for six-element Erfle eyepiece and hybrid eyepiece in Fig. 2(b) with  $\lambda = 555$  nm.

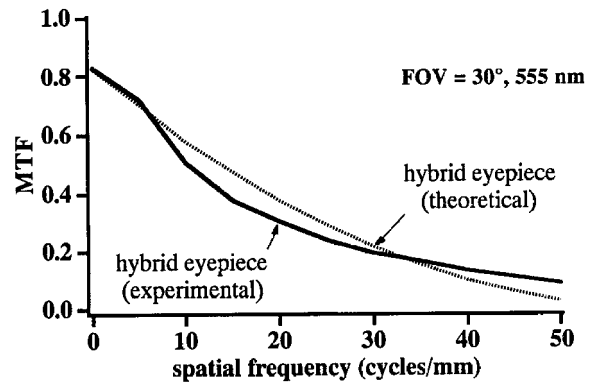


Fig. 10. Experimental and theoretical  $30^\circ$  full FOV MTF's for hybrid eyepiece in Fig. 2(b) with  $\lambda = 555$  nm.

The hybrid eyepiece was experimentally compared with a 20-mm FL Erfle eyepiece by the use of an Ealing MTF test bench; an infinite conjugate configuration on the eye side of the eyepiece was used. In the test setup, a 5-mm aperture stop was placed at the exit pupil location of each eyepiece (as shown in Figs. 1 and 2) so that the eyepieces were tested at  $f/4$ . The conventional refractive eyepiece used in the testing was a six-element Erfle eyepiece from Edmund Scientific Inc., in which the original patented design is modified by the replacement of the center element with a doublet. The additional lens in this commercial, Erfle-type eyepiece was added to improved the lateral color correction over that of the five-element design.

The first experiment performed was an on-axis test of the MTF at  $\lambda = 555$  nm. The experimental and the theoretical on-axis results for the hybrid eyepiece are shown in Fig. 8. Each data group is scaled by the measured integrated diffraction efficiency of the lens for the portion of the lens sampled. Light from specific regions of an object sample subaperture portions of the diffractive lens; therefore the efficiency values can be different for separate FOV's. The measured on-axis efficiency of the lens is 90%. The experimental on-axis MTF results for the Erfle eyepiece and for the hybrid eyepiece are shown plotted on the same graph in Fig. 9.

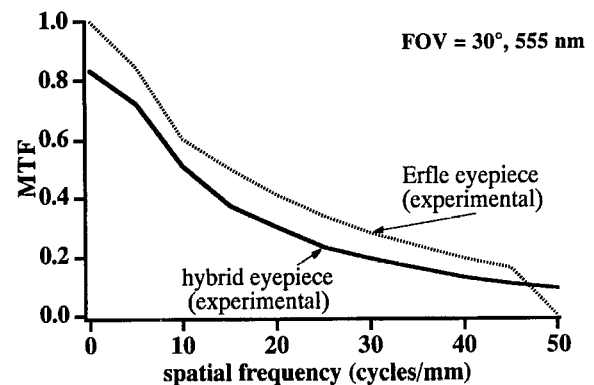


Fig. 11. Experimental  $30^\circ$  FOV MTF for six-element Erfle eyepiece and hybrid eyepiece in Fig. 2(b) with  $\lambda = 555$  nm.



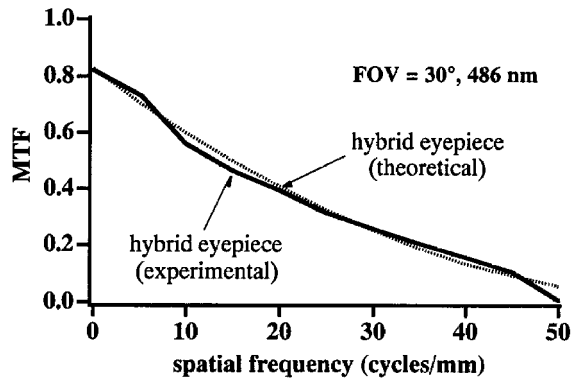


Fig. 12. Experimental and theoretical 30° FOV MTF's for hybrid eyepiece in Fig. 2(b) with  $\lambda = 486$  nm.

For off-axis MTF performance testing, the eyepieces were tested at 30° full FOV at  $\lambda = 555$  nm. Again the experimental and theoretical results for the hybrid eyepiece are compared in Fig. 10. The data are similarly scaled by the measured integrated diffraction efficiency of the sampled portion of the lens, which was 83%. Note that the diffractive element in the eyepiece was a prototype lens; further optimization of the blaze profile is expected to improve the integrated diffraction efficiency of the lens to a value approaching 97%–99%; this will directly raise the MTF curves by the increase in the efficiency. For ease of comparison, the experimental off-axis MTF results for the Erfle eyepiece and for the hybrid eyepiece are shown on the same graph in Fig. 11.

The experimental resolution performance of the hybrid eyepiece at both  $\lambda = 486$  nm and  $\lambda = 656$  nm also matches well with the theoretical performance. The experimental and the theoretical MTF data for 30° full FOV at  $\lambda = 486$  nm and  $\lambda = 656$  nm are plotted in Figs. 12 and 13, respectively. These data are also scaled by the measured, off-axis integrated diffraction efficiencies. For  $\lambda = 486$  nm, the off-axis efficiency is 82.2% (on-axis efficiency is 87%), and for  $\lambda = 656$  nm the off-axis efficiency is 70% (on-axis efficiency is 77%). The integrated efficiency used to scale the  $\lambda = 656$  nm MTF data was actually measured at  $\lambda = 632.8$  nm.

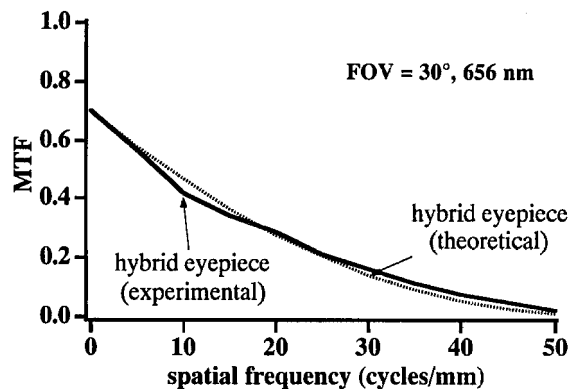


Fig. 13. Experimental and theoretical 30° FOV MTF's for hybrid eyepiece in Fig. 2(b) with  $\lambda = 656$  nm.

## 6. Summary and Discussion

We have demonstrated that hybrid diffractive–refractive wide-angle eyepiece designs can have comparable or improved performance compared with conventional wide-angle eyepieces, while simultaneously offering significant reductions in the weight, size, and number of elements of the design. Eyepiece design improvement in the past has been limited by several constraints of conventional design variables that are difficult to overcome. For example, the necessary elements added to designs for the correction of lateral color in conventional wide-angle eyepieces has led to more-complex, exotic solutions for wide-field aberration correction. Additionally, features of eyepieces, such as an external exit pupil and a wide-field angle, complicate the unique design. Many features of diffractive lenses match well with the requirements for eyepiece design and extend the possibilities for new eyepiece designs.

In our eyepieces we have used diffractive lenses to reduce the size and the weight of the system by employing their inherent strong color-correcting benefits and the ability to shape the emerging wave front. These new degrees of freedom allow one to design eyepieces with improved color correction, reduced field aberrations, and enhanced pupil imaging. The hybrid, three-element designs have reduced surface curvatures compared with those in the Erfle eyepiece and also employ only common crown glasses. The hybrid designs also allow larger apertures and increased field angles compared with conventional wide-angle eyepieces.

When diffractive optical elements are used in a visual (or any) optical system, the effects that are due to nonunity diffraction efficiency must be analyzed carefully. In particular, the energy in diffraction orders, other than the principal diffraction order, can result in undesirable multiple images (akin to ghost images) or can reduce contrast in the desired image (akin to veiling glare); hence it is extremely important to maximize the diffraction efficiency of the principal diffraction order. There are numerous factors that can affect the diffraction efficiency, including surface-blaze profile, zone spacing, surface coatings, illumination wavelength, incidence angle, polarization, and substrate index of refraction. When one investigates the suitability of a diffractive optics solution for a specific application, all these factors should be considered.

In the hybrid eyepiece described here, the diffractive lens element operates at  $f/10$  and its phase function contains an aspheric term. Because the diffractive element is rather strong ( $f/10$ ), any unwanted diffraction orders focus at a relatively large distance from the principal image plane; thus the main effect of nonunity diffraction efficiency in this case is to reduce the contrast of the resulting image. The aspheric contribution to the wave front produced by the diffractive element actually helps with regard to fabrication because it tends to increase the zone spacings at the edge of the aperture [e.g., the mini-

mum zone spacing for the diffractive element for the hybrid design shown in Fig. 2(b) is approximately 25  $\mu\text{m}$ , which is not particularly difficult to achieve with current fabrication techniques].

The diffraction efficiency at the design wavelength of 555 nm for the diffractive element used in the prototype hybrid eyepiece was found to be 90% for on-axis points and it dropped to 83% at an off-axis semifield angle of 15°. The dominant visual effect of nonunity diffraction efficiency is the reduction in image contrast. The effect of the nonunity diffraction efficiency on the experimental MTF curves is shown clearly in Figs. 8–13; the integrated diffraction efficiency serves as a scaling factor for the MTF.

Based on our preliminary observations, it appears that the image contrast obtained with diffractive–refractive hybrid lenses will be comparable with the image contrast observed in conventional all-refractive visual optical systems, provided that the integrated diffraction efficiency is above 95% at the design wavelength. Recent progress in fabrication techniques<sup>22</sup> have resulted in replicated diffractive elements operating in the visible spectrum that have an integrated diffraction efficiency at the design wavelength in the range from 97% to 99%; hence, we feel confident that diffractive optics can indeed play a significant role in visual optical systems.

This research was supported in part by the U.S. Army Research Office. The authors acknowledge the support of Rochester Photonics Corporation in providing the fabrication of the diffractive lens elements. Portions of this research were presented as paper JMC5 at the joint session of the OSA topical meeting of Diffractive Optics: Design, Fabrication, and Applications and the International Optical Design Conference of the Optical Society of America, Rochester, New York, 6–9 June, 1994.

## References

1. R. Kingslake, *Lens Design Fundamentals* (Academic, New York, 1978), pp. 335–336.
2. W. J. Smith, *Modern Lens Design* (McGraw-Hill, New York, 1992), pp. 87–88.
3. For examples of wide-angle eyepiece designs, see A. Cox, *A System of Optical Design* (Focal, New York, 1964), pp. 563–575.
4. H. Erfle, "Ocular," U.S. patent 1,478,704 (25 December 1923).
5. W. J. Smith, *Modern Optical Engineering*, 2nd ed. (McGraw-Hill, New York, 1990), pp. 404–407.
6. *Optical Design-Military Standardization Handbook MIL-HDBK-141* (Defense Supply Agency, Washington, D.C., 1962), p. 14–1.
7. See, for example, T. Stone and N. George, "Hybrid diffractive-refractive lenses and achromats," *Appl. Opt.* **27**, 2960–2971 (1988).
8. W. A. Kleinmans, "Aberrations of curved zone plates and Fresnel lenses," *Appl. Opt.* **16**, 1701–1704 (1977).
9. W. C. Sweatt, "Describing holographic optical elements as lenses," *J. Opt. Soc. Am.* **67**, 803–808 (1977).
10. D. A. Buralli and G. M. Morris, "Design of diffractive singlets for monochromatic imaging," *Appl. Opt.* **30**, 2151–2158 (1991).
11. S. Rosin, "Eyepieces and magnifiers," in *Applied Optics and Optical Engineering*, Vol. III of Optical Components, R. Kingslake, ed. (Academic, New York, 1965), p. 331–361.
12. R. W. Wood, "Phase-reversal zone-plates and diffraction-telescopes," *Philos. Mag.* **45**, 511–522 (1898).
13. S. J. Bennett, "Achromatic combinations of hologram optical elements," *Appl. Opt.* **15**, 542–545 (1976).
14. T. W. Stone, "Hybrid diffractive-refractive telescope," in *Practical Holography IV*, S. A. Benton, ed., *Proc. Soc. Photo-Opt. Instrum. Eng.* **1212**, 257–266 (1990).
15. C. W. Chen, "Binocular eyepiece optical system employing refractive and diffractive optical elements," U.S. patent 5,151,823 (29 September 1992).
16. R. E. Aldrich, "Ultra lightweight diffractive eyepiece, in *Diffractive Optics: Design, Fabrication, and Applications*, Vol. 9 of 1992 OSA Technical Digest Series (Optical Society of America, Washington, D.C., 1992), p. 129.
17. D. Williamson, "The eye in optical systems," in *Geometrical Optics*, R. E. Fischer, ed., *Proc. Soc. Photo-Opt. Instrum. Eng.* **531**, 136–147 (1985).
18. D. Sinclair, "Designing diffractive optics using the Sweatt model," *Sinclair Opt. Des. Notes* **1**(1), 1–3 (1990).
19. D. A. Buralli and G. M. Morris, "Effects of diffraction efficiency on the modulation transfer function of diffractive lenses," *Appl. Opt.* **31**, 4389–4396 (1992).
20. See, for example, D. A. Buralli, G. M. Morris, and J. R. Rogers, "Optical performance of holographic kinoforms," *Appl. Opt.* **28**, 967–983 (1989).
21. J. Bowen, C. G. Blough, and V. Wong, "Fabrication of optical surfaces by laser pattern generation," in *Optical Fabrication and Testing Workshop*, Vol. 13 of 1994 OSA Technical Digest Series (Optical Society of America, Washington, D.C., 1994), pp. 153–156.
22. G. Blough, Rochester Photonics Corporation, 330 Clay Road, Rochester, NY 14627 (private communication).